Robotics and Autonomous Systems 62 (2014) 1691–1701

Contents lists available at ScienceDirect

Robotics and Autonomous Systems

journal homepage: www.elsevier.com/locate/robot

Control of teleoperators with joint flexibility, uncertain parameters and time-delays☆

Emmanuel Nuño [a,*], Ioannis Sarras [b], Luis Basañez [c], Michel Kinnaert [d]

[a] Department of Computer Science, CUCEI, University of Guadalajara, Guadalajara, Mexico
[b] Automatic Control Department, SUPELEC, Gif-sur-Yvette, France
[c] Institute of Industrial and Control Engineering, Technical University of Catalonia, Barcelona, Spain
[d] Control Engineering and Systems Analysis Department, Université Libre de Bruxelles, Brussels, Belgium

ARTICLE INFO

Article history:
Received 23 July 2012
Received in revised form
25 October 2013
Accepted 11 August 2014
Available online 27 August 2014

Keywords:
Bilateral teleoperation
Uncertain parameters
Time-delays
Joint flexibility

ABSTRACT

The problem of controlling a rigid bilateral teleoperator has been the subject of study since the late 1980s and several control approaches have been reported to deal with time-delays, position tracking and transparency. However, the general flexible case is still an open problem. The present paper reports an adaptive and damping injection controller and a proportional plus damping injection ($P+d$) controller which are capable of globally stabilizing a nonlinear bilateral teleoperator with joint flexibility and time-delays. More precisely, the adaptive scheme is able to cope with uncertainty in the parameters and constant time-delays, while the $P+d$ scheme is shown to treat variable time-delays. In both cases, the teleoperator is composed of a rigid local manipulator and a flexible joint remote manipulator. The extension to the case where the local and remote manipulators exhibit joint flexibility is also reported using the $P+d$ scheme. Under the common assumption that the human operator and the environment are passive it is proven, for the $P+d$ schemes, that the joint and actuator velocities as well as the local and remote position errors are bounded. Moreover, if the human operator and remote environment forces are zero then, for both controllers, position tracking is established and local and remote velocities asymptotically converge to zero. Simulations and experiments are presented to depict the performance of the proposed schemes.

1. Introduction

A teleoperator is composed of a *human operator*, a *local manipulator*, a *communication channel*, a *remote manipulator* and a remote *environment*. The main objective of such a scheme is to extend the human manipulation capabilities to a remote environment. To this end, the local and remote manipulators exchange control signals through the communication channel and the remote force interaction is reflected back to the operator. Controlling these systems has become a highly active research field. For a historical survey on this research line the reader may refer to [1] and, for a tutorial on teleoperators control, to [2].

Since its introduction, by Anderson and Spong [3] in the late 1980s, the scattering transformation has dominated the field of teleoperators control. However, one of the issues with most of the scattering-based schemes is position drift (an exception is reported in [4]). Recently, Chopra et al. [5] have proposed the use of adaptive schemes to overcome the effects of position drift, without the use of the scattering transformation. Along the same line Nuño et al. [6] have reported a different adaptive scheme capable of synchronizing the local and remote positions despite constant time-delays, with a corrected proof reported in [7]. In [8] the adaptive controller of [6] is extended to the synchronization of multiple robot networks with delays. Other remarkable adaptive schemes for rigid joint manipulators can be found in [9–11].

On the other hand, Lee and Spong [12] suggest the use of a proportional-derivative plus damping controller to control a teleoperator with constant time-delays. Later, in [13], for the constant time-delay case, and in [14], for the variable time-delay case, Nuño et al. show that simple proportional plus damping ($P+d$)

☆ This work has been partially supported by the Mexican projects CONACyT CB-129079 and INFR-229696 and the Spanish CICYT projects DPI2010-15446 and DPI2011-22471. Support by the IAP Programme initiated by the Belgian State, Science Policy Office, through the Belgian Network DYSCO is gratefully acknowledged. The scientific responsibility rests with the authors.
* Corresponding author. Tel.: +52 33 13785900x27748.
E-mail addresses: emmanuel.nuno@cucei.udg.mx (E. Nuño), sarras@ieee.org (I. Sarras), luis.basanez@upc.edu (L. Basañez), Michel.Kinnaert@ulb.ac.be (M. Kinnaert).

http://dx.doi.org/10.1016/j.robot.2014.08.003
0921-8890/

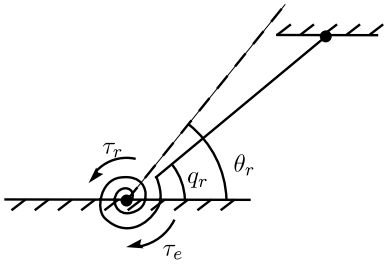

Fig. 1. One-DOF manipulator with a flexible joint.

controllers are capable of providing position tracking in delayed teleoperators. All these previous schemes analyze the case when the local and remote manipulators are composed of rigid links. Nevertheless, it should be underscored that in diverse applications, including space and surgical telerobotics, the use of thin, lightweight, flexible and cable-driven manipulators is increasing [15]. Despite this, most of the teleoperator controllers reported until today only deal with rigid manipulators. Few exceptions, for linearized teleoperators and without time-delays, are [16–20]. A remarkable work has been recently reported in [21] where the authors present a full-state feedback controller for the teleoperation of flexible joint manipulators without delays.

The present work reports some first results on the control of nonlinear teleoperators with joint flexibility, uncertainty in the parameters and time-delays. In particular, two different controllers are presented: an asymmetric adaptive and damping injection controller that deals with uncertainty in the plant parameters and constant time-delays, and a symmetric proportional plus damping controller that is robust to variable time-delays. Compared to our previous work [22], this paper reports the asymmetric controller and provides a more thorough presentation of the proposed control schemes. In particular, it is proven that, if the human operator does not inject forces on the local manipulator, then velocities and position error globally asymptotically converge to zero. The proofs of such properties employ formal arguments based on Barbalăt's Lemma. Another contribution consists of the proof that the proportional plus damping controller ensures global convergence of the velocities and position error to zero, when both local and remote manipulators exhibit joint flexibility. It should be underscored that, for flexible manipulators, the reported schemes do not need the complete state, joint and link positions and velocities, to be measured nor the human/environment forces. Only the joint (actuator) part of the state appears explicitly in the control law.

1.1. Notation

To streamline the presentation throughout the paper the following notation is introduced. Lower case letters denote scalar functions, *e.g.* t, bold lower case letters denote vector functions, *e.g.* $\mathbf{x}$, and bold upper case letters denote matrices, *e.g.* $\mathbf{A}$. Additionally, $\mathbb{R} := (-\infty, \infty)$, $\mathbb{R}_{>0} := (0, \infty)$, $\mathbb{R}_{\geq 0} := [0, \infty)$. $\lambda_m\{\mathbf{A}\}$ and $\lambda_M\{\mathbf{A}\}$ represent the minimum and maximum eigenvalues of matrix $\mathbf{A}$, respectively, while $\|\mathbf{A}\|$ denotes the matrix-induced 2-norm. $|\mathbf{x}|$ stands for the standard Euclidean norm of vector $\mathbf{x}$. For any function $\mathbf{f} : \mathbb{R}_{\geq 0} \to \mathbb{R}^n$, the $\mathcal{L}_\infty$-norm is defined as $\|\mathbf{f}\|_\infty := \sup_{t\geq 0} |\mathbf{f}(t)|$, and the square of the $\mathcal{L}_2$-norm as $\|\mathbf{f}\|_2^2 := \int_0^\infty |\mathbf{f}(t)|^2 dt$. The $\mathcal{L}_\infty$ and $\mathcal{L}_2$ spaces are defined as the sets $\{\mathbf{f} : \mathbb{R}_{\geq 0} \to \mathbb{R}^n : \|\mathbf{f}\|_\infty < \infty\}$ and $\{\mathbf{f} : \mathbb{R}_{\geq 0} \to \mathbb{R}^n : \|\mathbf{f}\|_2 < \infty\}$, respectively.

2. Modeling the teleoperator with remote flexibility

Let us assume that gravity is compensated in both the local and remote manipulators. Then the local manipulator is modeled as an n-degree of freedom (DOF) manipulator with rigid joints. Its nonlinear dynamic behavior is given by

$$\mathbf{M}_l(\mathbf{q}_l)\ddot{\mathbf{q}}_l + \mathbf{C}_l(\mathbf{q}_l, \dot{\mathbf{q}}_l)\dot{\mathbf{q}}_l = \boldsymbol{\tau}_h - \boldsymbol{\tau}_l. \tag{1}$$

The remote manipulator is assumed to be an n-DOF manipulator with flexible joints (Fig. 1 shows, schematically, a manipulator with one revolute DOF), whose dynamical behavior is governed by [23,24]

$$\mathbf{M}_r(\mathbf{q}_r)\ddot{\mathbf{q}}_r + \mathbf{C}_r(\mathbf{q}_r, \dot{\mathbf{q}}_r)\dot{\mathbf{q}}_r + \mathbf{S}_r[\mathbf{q}_r - \boldsymbol{\theta}_r] = -\boldsymbol{\tau}_e \tag{2a}$$

$$\mathbf{J}_r\ddot{\boldsymbol{\theta}}_r + \mathbf{S}_r[\boldsymbol{\theta}_r - \mathbf{q}_r] = \boldsymbol{\tau}_r \tag{2b}$$

where, using the subindex $i \in \{l, r\}$ for local and remote manipulators, respectively, $\mathbf{q}_i \in \mathbb{R}^n$ is the link position and $\boldsymbol{\theta}_r \in \mathbb{R}^n$ is the remote joint (motor) position, $\mathbf{M}_i(\mathbf{q}_i) \in \mathbb{R}^{n\times n}$ is the symmetric inertia matrix, $\mathbf{C}_i(\mathbf{q}_i, \dot{\mathbf{q}}_i) \in \mathbb{R}^{n\times n}$ is the Coriolis and centrifugal effects matrix, defined via the Christoffel symbols of the first kind, $\mathbf{J}_r \in \mathbb{R}^{n\times n}$ is a constant diagonal matrix representing the remote actuator moments of inertia, $\mathbf{S}_r \in \mathbb{R}^{n\times n}$ is a constant diagonal and positive definite matrix that contains the remote joint stiffness, $\boldsymbol{\tau}_i \in \mathbb{R}^n$ is the control signal and $\boldsymbol{\tau}_h \in \mathbb{R}^n$, $\boldsymbol{\tau}_e \in \mathbb{R}^n$ are the joint torques corresponding to the forces exerted by the human operator and the environment interaction, respectively.

It is further assumed that the manipulators are serial chains with a certain combination of revolute and prismatic joints such that the inertia matrix is lower and upper bounded (*cf.* [25–27]). Under these assumptions, dynamics (1) and (2a) enjoy the following properties [28,29,14]:

P1. $\forall\, \mathbf{q}_i \in \mathbb{R}^n$, $\exists m_i, M_i \in \mathbb{R}_{>0}$ such that $m_i \leq \|\mathbf{M}_i(\mathbf{q}_i)\| \leq M_i$.
P2. Matrix $\dot{\mathbf{M}}_i(\mathbf{q}_i) - 2\mathbf{C}_i(\mathbf{q}_i, \dot{\mathbf{q}}_i)$ is skew-symmetric.
P3. $\forall\, \mathbf{q}_i, \dot{\mathbf{q}}_i \in \mathbb{R}^n$, $\exists c_i \in \mathbb{R}_{>0}$ such that $|\mathbf{C}_i(\mathbf{q}_i, \dot{\mathbf{q}}_i)\dot{\mathbf{q}}_i| \leq c_i|\dot{\mathbf{q}}_i|^2$.
P4. If $\dot{\mathbf{q}}_i, \ddot{\mathbf{q}}_i \in \mathcal{L}_\infty$ then $\frac{d}{dt}\mathbf{C}_i(\mathbf{q}_i, \dot{\mathbf{q}}_i)$ is a bounded operator.
P5. $\forall\, \mathbf{x}, \mathbf{y} \in \mathbb{R}^n$, the dynamics (1) are linearly parameterizable as $\mathbf{M}_l(\mathbf{q}_l)\mathbf{x} + \mathbf{C}_l(\mathbf{q}_l, \dot{\mathbf{q}}_l)\mathbf{y} = \mathbf{Y}(\mathbf{q}_l, \dot{\mathbf{q}}_l, \mathbf{x}, \mathbf{y})\boldsymbol{\phi}_l$, where $\mathbf{Y}_l(\mathbf{q}_l, \dot{\mathbf{q}}_l, \mathbf{x}, \mathbf{y}) \in \mathbb{R}^{n\times p}$ is a regressor matrix of known functions and $\boldsymbol{\phi}_l \in \mathbb{R}^p$ is a constant vector function of the manipulator physical parameters (link masses, moments of inertia, etc.).

Remark 1. It is well-known that (1) satisfies the power-balance equation $\dot{V}_l = \dot{\mathbf{q}}_l^\top(\boldsymbol{\tau}_h - \boldsymbol{\tau}_l)$, where $V_l(\mathbf{q}_l, \dot{\mathbf{q}}_l) = \frac{1}{2}\dot{\mathbf{q}}_l^\top\mathbf{M}_l(\mathbf{q}_l)\dot{\mathbf{q}}_l \geq 0$. Furthermore, (2) satisfies $\dot{V}_r = -\dot{\mathbf{q}}_l^\top\boldsymbol{\tau}_e + \dot{\boldsymbol{\theta}}_r^\top\boldsymbol{\tau}_r$ where

$$V_r(\mathbf{q}_r, \dot{\mathbf{q}}_r, \boldsymbol{\theta}_r, \dot{\boldsymbol{\theta}}_r) = \frac{1}{2}\left(\dot{\mathbf{q}}_r^\top\mathbf{M}_r(\mathbf{q}_r)\dot{\mathbf{q}}_r + \dot{\boldsymbol{\theta}}_r^\top\mathbf{J}_r\dot{\boldsymbol{\theta}}_r + (\mathbf{q}_r - \boldsymbol{\theta}_r)^\top\mathbf{S}_r(\mathbf{q}_r - \boldsymbol{\theta}_r)\right). \tag{3}$$

Remark 2. The controllers proposed in the following sections assume that only joint (motor) positions and velocities are available for measurement.

3. The adaptive controller for constant delays

In this section the time-delays are assumed constant. In this scenario the local and remote joint position errors are defined as

$$\mathbf{e}_l := \mathbf{q}_l - \boldsymbol{\theta}_r(t - T_r), \qquad \mathbf{e}_r := \boldsymbol{\theta}_r - \mathbf{q}_l(t - T_l), \tag{4}$$

and, for convenience, let us also define the following signal

$$\boldsymbol{\epsilon}_l = \dot{\mathbf{q}}_l + \lambda\mathbf{e}_l, \tag{5}$$

where $\lambda \in \mathbb{R}_{>0}$ is a control gain.

Considering that the local manipulator is composed of rigid joints, the adaptive scheme proposed in [6] is employed to ensure position tracking. The adopted controller is then given by

$$\boldsymbol{\tau}_l = \lambda\hat{\mathbf{M}}_l(\mathbf{q}_l)\dot{\mathbf{e}}_l + \lambda\hat{\mathbf{C}}_l(\mathbf{q}_l, \dot{\mathbf{q}}_l)\mathbf{e}_l + \mathbf{K}_l\boldsymbol{\epsilon}_l + \mathbf{B}\dot{\mathbf{e}}_l \tag{6}$$

where $\mathbf{K}_l, \mathbf{B} \in \mathbb{R}^{n\times n}$ are symmetric positive definite matrices and $\hat{\mathbf{M}}_l$, $\hat{\mathbf{C}}_l$ stand for the matrix estimations of $\mathbf{M}_l$ and $\mathbf{C}_l$, respectively.

Using Property P5, we can write $\mathbf{Y}_l(\mathbf{q}_l, \dot{\mathbf{q}}_l, \dot{\mathbf{e}}_l, \mathbf{e}_l)\hat{\boldsymbol{\phi}}_l = \lambda\hat{\mathbf{M}}_l(\mathbf{q}_l)\dot{\mathbf{e}}_l + \lambda\hat{\mathbf{C}}_l(\mathbf{q}_l, \dot{\mathbf{q}}_l)\mathbf{e}_l$. Thus, the local controller can be further written as

$$\boldsymbol{\tau}_l = \mathbf{Y}_l(\mathbf{q}_l, \dot{\mathbf{q}}_l, \dot{\mathbf{e}}_l, \mathbf{e}_l)\hat{\boldsymbol{\phi}}_l + \mathbf{K}_l\boldsymbol{\epsilon}_l + \mathbf{B}\dot{\mathbf{e}}_l.$$

Substituting the controller (6) in the local manipulator dynamics (1), and using (5), yields

$$\mathbf{M}_l(\mathbf{q}_l)\dot{\boldsymbol{\epsilon}}_l + [\mathbf{C}_l(\mathbf{q}_l, \dot{\mathbf{q}}_l) + \mathbf{K}_l]\boldsymbol{\epsilon}_l + \mathbf{B}\dot{\mathbf{e}}_l = \mathbf{Y}_l\tilde{\boldsymbol{\phi}}_l + \boldsymbol{\tau}_h, \tag{7}$$

with $\tilde{\boldsymbol{\phi}}_l = \boldsymbol{\phi}_l - \hat{\boldsymbol{\phi}}_l$, the estimation error. The dynamics of the estimated uncertain parameters are given by

$$\dot{\tilde{\boldsymbol{\phi}}}_l = -\dot{\hat{\boldsymbol{\phi}}}_l = -\boldsymbol{\Gamma}_l\mathbf{Y}_l^\top\boldsymbol{\epsilon}_l, \tag{8}$$

where it is used the fact that $\dot{\boldsymbol{\phi}}_l = \mathbf{0}$ and $\boldsymbol{\Gamma}_l \in \mathbb{R}^{p\times p}$ is a symmetric positive definite matrix. It is worth mentioning that other estimation laws, like the gradient algorithm with projection, can improve the parameter estimation performance. For a detailed survey along this line, the reader may refer to [30].

For the remote manipulator, the proposed controller is

$$\boldsymbol{\tau}_r = -\lambda\mathbf{B}\dot{\mathbf{e}}_r - \mathbf{K}_r\dot{\boldsymbol{\theta}}_r, \tag{9}$$

where the control gain $\mathbf{K}_r \in \mathbb{R}^{n\times n}$ is diagonal and positive definite. Note that $\dot{\mathbf{e}}_r = \dot{\boldsymbol{\theta}}_r - \dot{\mathbf{q}}_l(t - T_l)$. Now, the first contribution of this paper can be stated.

Proposition 1. *Consider the bilateral teleoperator dynamics (1)–(2) in closed-loop with the controllers (6), (8) and (9) for any constant time-delay T_i. Then,*

i. *if the human operator force is bounded, i.e., $\boldsymbol{\tau}_h \in \mathcal{L}_\infty$ and the remote environment force is passive from velocity to force, i.e., there exists $\kappa_r \in \mathbb{R}_{\geq 0}$ such that, for all $t \geq 0$, $\int_0^t \dot{\mathbf{q}}_r^\top(\sigma)\boldsymbol{\tau}_e(\sigma)d\sigma + \kappa_r \geq 0$, then $\boldsymbol{\epsilon}_l$, $\dot{\mathbf{e}}_i$ and $\dot{\boldsymbol{\theta}}_r$ are bounded.*
ii. *if the human operator and the environment forces are zero, i.e., $\boldsymbol{\tau}_h = \boldsymbol{\tau}_e = \mathbf{0}$, all velocity signals and position errors in the system are bounded and asymptotically converge to zero, i.e., $|\mathbf{q}_l - \mathbf{q}_r|$, $|\mathbf{q}_r - \boldsymbol{\theta}_r|$, $|\dot{\mathbf{q}}_l|$, $|\dot{\boldsymbol{\theta}}_r| \to 0$ as $t \to \infty$.*

Proof. Consider the following Lyapunov–Krasovskiĭ functional, $U_l(\boldsymbol{\epsilon}_l, \mathbf{e}_l, \tilde{\boldsymbol{\phi}}_l, t)$,

$$U_l = \frac{1}{2}\left(\boldsymbol{\epsilon}_l^\top\mathbf{M}_l\boldsymbol{\epsilon}_l + \lambda\mathbf{e}_l^\top\mathbf{B}\mathbf{e}_l + \lambda\int_{t-T_l}^t \dot{\mathbf{q}}_l^\top\mathbf{B}\dot{\mathbf{q}}_l d\sigma + \tilde{\boldsymbol{\phi}}_l^\top\boldsymbol{\Gamma}_l^{-1}\tilde{\boldsymbol{\phi}}_l + \lambda\int_{t-T_r}^t \dot{\boldsymbol{\theta}}_r^\top\mathbf{B}\dot{\boldsymbol{\theta}}_r d\sigma\right).$$

U_l is positive definite and radially unbounded with respect to $\boldsymbol{\epsilon}_l$, $\mathbf{e}_l$, $\tilde{\boldsymbol{\phi}}_l$, and its time-derivative along (7) and (8) is given by

$$\dot{U}_l = -\frac{\lambda}{2}\left[\dot{\mathbf{e}}_l^\top\mathbf{B}\dot{\mathbf{e}}_l - \dot{\boldsymbol{\theta}}_r^\top\mathbf{B}\dot{\boldsymbol{\theta}}_r + \dot{\mathbf{q}}_l^\top(t - T_l)\mathbf{B}\dot{\mathbf{q}}_l(t - T_l)\right] - \boldsymbol{\epsilon}_l^\top\mathbf{K}_l\boldsymbol{\epsilon}_l + \boldsymbol{\epsilon}_l^\top\boldsymbol{\tau}_h,$$

where Property P2 and (5) have been used to eliminate some crossed terms.

Now, defining $U := U_l + V_r + \int_0^t \dot{\mathbf{q}}_r^\top(\sigma)\boldsymbol{\tau}_e(\sigma)d\sigma + \kappa_r$, with V_r defined in (3), yields $\dot{U} = \dot{U}_l + \dot{\boldsymbol{\theta}}_r^\top\boldsymbol{\tau}_r$. Substituting (9) in $\dot{U}$, it can be easily proved that

$$\dot{U} = -\boldsymbol{\epsilon}_l^\top\mathbf{K}_l\boldsymbol{\epsilon}_l - \dot{\boldsymbol{\theta}}_r^\top\mathbf{K}_r\dot{\boldsymbol{\theta}}_r - \frac{\lambda}{2}\dot{\mathbf{e}}_l^\top\mathbf{B}\dot{\mathbf{e}}_l - \frac{\lambda}{2}\dot{\mathbf{e}}_r^\top\mathbf{B}\dot{\mathbf{e}}_r + \boldsymbol{\epsilon}_l^\top\boldsymbol{\tau}_h.$$

Using Young's inequality on the crossed term $\boldsymbol{\epsilon}_l^\top\boldsymbol{\tau}_h$ yields

$$\dot{U} \leq -\frac{k_l}{2}|\boldsymbol{\epsilon}_l|^2 - \dot{\boldsymbol{\theta}}_r^\top\mathbf{K}_r\dot{\boldsymbol{\theta}}_r - \frac{\lambda}{2}\dot{\mathbf{e}}_l^\top\mathbf{B}\dot{\mathbf{e}}_l - \frac{\lambda}{2}\dot{\mathbf{e}}_r^\top\mathbf{B}\dot{\mathbf{e}}_r + \frac{1}{2k_l}|\boldsymbol{\tau}_h|^2,$$

where $k_l := \lambda_m\{\mathbf{K}_l\}$. The proof of Part (i) follows directly from the fact that $U \geq 0$ and $\boldsymbol{\tau}_h \in \mathcal{L}_\infty$.

For the proof of part (ii), $\boldsymbol{\tau}_h$ and $\boldsymbol{\tau}_r$ are set to zero. In this case,

$$\dot{U} = -\boldsymbol{\epsilon}_l^\top\mathbf{K}_l\boldsymbol{\epsilon}_l - \dot{\boldsymbol{\theta}}_r^\top\mathbf{K}_r\dot{\boldsymbol{\theta}}_r - \frac{\lambda}{2}\dot{\mathbf{e}}_l^\top\mathbf{B}\dot{\mathbf{e}}_l - \frac{\lambda}{2}\dot{\mathbf{e}}_r^\top\mathbf{B}\dot{\mathbf{e}}_r.$$

The fact that $U \geq 0$ and $\dot{U} \leq 0$ ensures that $\boldsymbol{\epsilon}_l, \dot{\boldsymbol{\theta}}_r, \dot{\mathbf{e}}_i \in \mathcal{L}_2$ and $\boldsymbol{\epsilon}_l, \mathbf{e}_l, \tilde{\boldsymbol{\phi}}_l, \dot{\boldsymbol{\theta}}_r, \dot{\mathbf{q}}_r, |\mathbf{q}_r - \boldsymbol{\theta}_r| \in \mathcal{L}_\infty$. Now, $\boldsymbol{\epsilon}_l, \mathbf{e}_l \in \mathcal{L}_\infty$ ensures that $\dot{\mathbf{q}}_l \in \mathcal{L}_\infty$. All these bounded signals imply, from (7), that $\dot{\boldsymbol{\epsilon}}_l \in \mathcal{L}_\infty$. This last, together with $\boldsymbol{\epsilon}_l \in \mathcal{L}_2 \cap \mathcal{L}_\infty$, support (using Barbalăt's Lemma) that $\lim_{t\to\infty}|\boldsymbol{\epsilon}_l(t)| = 0$. Moreover, $\dot{\boldsymbol{\theta}}_r, \dot{\mathbf{q}}_r, |\mathbf{q}_r - \boldsymbol{\theta}_r| \in \mathcal{L}_\infty$ also implies that $\ddot{\boldsymbol{\theta}}_r \in \mathcal{L}_\infty$; this in turn ensures – with the additional fact that $\dot{\boldsymbol{\theta}}_r \in \mathcal{L}_2 \cap \mathcal{L}_\infty$ – that $\lim_{t\to\infty}|\dot{\boldsymbol{\theta}}_r(t)| = 0$.

Now, using (5), we can write

$$\dot{\mathbf{e}}_l = -\lambda\mathbf{e}_l + \mathbf{u}_l \tag{10}$$

where $\mathbf{u}_l := \boldsymbol{\epsilon}_l - \dot{\boldsymbol{\theta}}_r(t - T_r)$. Note that (10) represents an asymptotically stable map, $\mathbf{u}_l \to \mathbf{e}_l$, with an input in $\mathcal{L}_2 \cap \mathcal{L}_\infty$; hence $|\mathbf{e}_l| \to 0$. This last and convergence of $\dot{\boldsymbol{\theta}}_r, \boldsymbol{\epsilon}_l$ to zero, imply that $|\dot{\mathbf{e}}_l| \to 0$.

The rest of the proof can be easily established by proving that $\frac{d}{dt}\ddot{\boldsymbol{\theta}}_r \in \mathcal{L}_\infty$ and that $\lim_{t\to\infty}\int_0^t \ddot{\boldsymbol{\theta}}_r(\sigma)d\sigma$ is bounded and exists, which in turn implies that $\lim_{t\to\infty}\ddot{\boldsymbol{\theta}}_r(t) = \mathbf{0}$. The claim follows from the closed-loop actuator dynamics (2b), (9) and convergence of $\ddot{\boldsymbol{\theta}}_r, \dot{\boldsymbol{\theta}}_r, \dot{\mathbf{e}}_r$ to zero. ◁

Remark 3. Using the local controller (6) and the remote controller $\boldsymbol{\tau}_r = -\lambda\mathbf{B}\dot{\mathbf{e}}_r$, it can also be shown that the teleoperator (1), (2) is globally stable. Moreover, it can be proved – using the same functional U as in the previous proof – that velocity errors asymptotically converge to zero. These same conclusions hold if (6) is replaced by $\boldsymbol{\tau}_l = -\lambda\mathbf{B}\dot{\mathbf{e}}_l$. In this case, the Lyapunov–Krasovskiĭ functional is given by

$$U = V_l + V_r + \frac{1}{2}\int_{t-T_l}^t \dot{\mathbf{q}}_l^\top(\sigma)\mathbf{B}\dot{\mathbf{q}}_l(\sigma)d\sigma + \frac{1}{2}\int_{t-T_r}^t \dot{\boldsymbol{\theta}}_r^\top(\sigma)\mathbf{B}\dot{\boldsymbol{\theta}}_r(\sigma)d\sigma$$

where V_l and V_r are defined in Remark 1.

4. The variable time-delays case

In the rest of the paper, it is assumed that the time-delays in the communication channel, the human operator and the environment satisfy the following:

A1. The variable time-delays $T_i(t)$ have known upper bounds ${}^*T_i$, i.e., $0 \leq T_i(t) \leq {}^*T_i < \infty$.
A2. The human operator and the environment define passive (velocity to force) maps, that is, there exists $\kappa_i \in \mathbb{R}_{\geq 0}$ such that, for all $t \geq 0$,

$$E_h := -\int_0^t \dot{\mathbf{q}}_l^\top(\sigma)\boldsymbol{\tau}_h(\sigma)d\sigma + \kappa_l \geq 0, \tag{11a}$$

$$E_e := \int_0^t \dot{\mathbf{q}}_r^\top(\sigma)\boldsymbol{\tau}_e(\sigma)d\sigma + \kappa_r \geq 0. \tag{11b}$$

Correspondingly, the position errors defined in (4) change to

$$\mathbf{e}_l = \mathbf{q}_l - \boldsymbol{\theta}_r(t - T_r(t)), \qquad \mathbf{e}_r = \boldsymbol{\theta}_r - \mathbf{q}_l(t - T_l(t)) \tag{12}$$

4.1. Symmetric P + d controller

Suppose that the control forces applied on the local and remote manipulators are proportional to their position errors plus a

damping injection term. In this scenario the control laws are given by[1]

$$\boldsymbol{\tau}_l = K_l \mathbf{e}_l + B_l \dot{\mathbf{q}}_l \tag{13a}$$

$$\boldsymbol{\tau}_r = -K_r \mathbf{e}_r - B_r \dot{\boldsymbol{\theta}}_r \tag{13b}$$

where K_i and B_i are positive constants.[2]

Before going through the stability properties, a lemma that is instrumental in the analysis is presented for completeness. Its proof can be found in [14].

Lemma 1. *For any vector signals $\mathbf{x}, \mathbf{y} \in \mathbb{R}^n$, any variable time-delay $0 \leq T(t) \leq {}^*T < \infty$ and any constant $\alpha > 0$, the following inequality holds*

$$-\int_0^t \mathbf{x}^\top(\sigma) \int_{-T(\sigma)}^0 \mathbf{y}(\sigma+\theta)\, d\theta\, d\sigma \leq \frac{\alpha}{2}\|\mathbf{x}\|_2^2 + \frac{{}^*T^2}{2\alpha}\|\mathbf{y}\|_2^2. \quad \diamond$$

Proposition 2. *Consider the teleoperator (1)–(2), controlled by (13) with $\boldsymbol{\tau}_h$, $\boldsymbol{\tau}_e$ verifying (11). Set the control gains such that*

$$4B_lB_r > ({}^*T_l + {}^*T_r)^2 K_l K_r \tag{14}$$

Then:

I. *Velocities and position errors are bounded, i.e., $\dot{\mathbf{q}}_i, \dot{\boldsymbol{\theta}}_r, \mathbf{q}_l - \mathbf{q}_r, \mathbf{q}_i - \boldsymbol{\theta}_r \in \mathcal{L}_\infty$. Moreover, $\dot{\mathbf{q}}_l, \dot{\boldsymbol{\theta}}_r \in \mathcal{L}_2$ and $|\ddot{\boldsymbol{\theta}}_r|, |\dot{\boldsymbol{\theta}}_r| \to 0$ as $t \to \infty$.*

II. *If additionally, the human operator and the environment do not inject any forces on the local and the remote manipulators, i.e. $\boldsymbol{\tau}_h = \boldsymbol{\tau}_e = \mathbf{0}$, the local and remote link position error and remote joint and actuator position error asymptotically converge to zero, i.e.,*

$$\lim_{t\to\infty} |\mathbf{q}_l(t) - \mathbf{q}_r(t)| = 0$$

and

$$\lim_{t\to\infty} |\mathbf{q}_r(t) - \boldsymbol{\theta}_r(t)| = 0.$$

Proof. Consider the function $V(\mathbf{q}_i, \dot{\mathbf{q}}_i, \boldsymbol{\theta}_r, \dot{\boldsymbol{\theta}}_r, t)$ given by

$$V = V_l + \frac{K_l}{K_r} V_r + E_h + \frac{K_l}{K_r} E_e + \frac{K_l}{2}|\mathbf{q}_l - \boldsymbol{\theta}_r|^2$$

where V_i are defined in Remark 1 and E_h and E_e in (11a) and (11b), respectively. Note that V is positive semi-definite and radially unbounded with regard to $\dot{\mathbf{q}}_i, \dot{\boldsymbol{\theta}}_r, |\mathbf{q}_r - \boldsymbol{\theta}_r|$ and $|\mathbf{q}_l - \boldsymbol{\theta}_r|$. Calculating its time-derivative along (1), (2) and using Property P2, yields

$$\dot{V} = -\dot{\mathbf{q}}_l^\top \boldsymbol{\tau}_l + \frac{K_l}{K_r}\dot{\boldsymbol{\theta}}_r^\top \boldsymbol{\tau}_r + K_l(\mathbf{q}_l - \boldsymbol{\theta}_r)^\top(\dot{\mathbf{q}}_l - \dot{\boldsymbol{\theta}}_r).$$

Substituting the controllers (13), we get

$$\begin{aligned}\dot{V} &= -B_l|\dot{\mathbf{q}}_l|^2 - K_l\dot{\mathbf{q}}_l^\top[\boldsymbol{\theta}_r - \boldsymbol{\theta}_r(t - T_r(t))] \\ &\quad - \frac{K_lB_r}{K_r}|\dot{\boldsymbol{\theta}}_r|^2 - K_l\dot{\boldsymbol{\theta}}_r^\top[\mathbf{q}_l - \mathbf{q}_l(t - T_l(t))],\end{aligned}$$

Noting that, for any $\mathbf{x} \in \mathbb{R}^n$,

$$\mathbf{x} - \mathbf{x}(t - T(t)) = \int_{-T(t)}^0 \dot{\mathbf{x}}(t+\sigma)\, d\sigma, \tag{15}$$

$\dot{V}$ can be written as

$$\begin{aligned}\dot{V} &= -B_l|\dot{\mathbf{q}}_l|^2 - K_l\dot{\mathbf{q}}_l^\top \int_{-T_r(t)}^0 \dot{\boldsymbol{\theta}}_r(t+\sigma)\, d\sigma \\ &\quad - \frac{K_lB_r}{K_r}|\dot{\boldsymbol{\theta}}_r|^2 - K_l\dot{\boldsymbol{\theta}}_r^\top \int_{-T_l(t)}^0 \dot{\mathbf{q}}_l(t+\sigma)\, d\sigma.\end{aligned}$$

Integrating from 0 to t, and invoking Lemma 1 on the above integral terms, with α_l and α_r, respectively, yields

$$\begin{aligned}V(t) - V(0) \leq &-\left[B_l - \frac{K_l}{2}\left(\alpha_l + \frac{{}^*T_l^2}{\alpha_r}\right)\right]\|\dot{\mathbf{q}}_l\|_2^2 \\ &-\left[\frac{K_lB_r}{K_r} - \frac{K_l}{2}\left(\alpha_r + \frac{{}^*T_r^2}{\alpha_l}\right)\right]\|\dot{\boldsymbol{\theta}}_r\|_2^2.\end{aligned}$$

Let us define $\lambda_i \in \mathbb{R}$ as

$$\lambda_l := B_l - \frac{K_l}{2}\left(\alpha_l + \frac{{}^*T_l^2}{\alpha_r}\right)$$

and

$$\lambda_r := B_r - \frac{K_r}{2}\left(\alpha_r + \frac{{}^*T_r^2}{\alpha_l}\right).$$

Note that if there exist $\lambda_i > 0$ then $\lambda_l\|\dot{\mathbf{q}}_l\|_2^2 + \frac{K_l}{K_r}\lambda_r\|\dot{\boldsymbol{\theta}}_r\|_2^2 \leq V(0)$; thus $\dot{\mathbf{q}}_l, \dot{\boldsymbol{\theta}}_r \in \mathcal{L}_2$.

Solving simultaneously for $\lambda_i > 0$ and $\alpha_i > 0$, there will exist a solution if $4B_lB_r > ({}^*T_l + {}^*T_r)^2K_lK_r$. Thus, setting the control gains fulfilling this last inequality ensures that $\exists \alpha_i > 0$ such that $\lambda_i > 0$ and $\dot{\mathbf{q}}_l, \dot{\boldsymbol{\theta}}_r \in \mathcal{L}_2$, which in turn implies that $V(t) \leq V(0)$. Hence $\dot{\mathbf{q}}_i$, $\dot{\boldsymbol{\theta}}_r$, $|\mathbf{q}_r - \boldsymbol{\theta}_r|$, $|\mathbf{q}_l - \boldsymbol{\theta}_r| \in \mathcal{L}_\infty$ which also implies that $|\mathbf{q}_l - \mathbf{q}_r| \in \mathcal{L}_\infty$.

In order to prove that $\lim_{t\to\infty}|\dot{\boldsymbol{\theta}}_r(t)| = 0$, let us rewrite $\boldsymbol{\tau}_r$ as

$$\boldsymbol{\tau}_r = K_r(\mathbf{q}_l - \boldsymbol{\theta}_r) - B_r\dot{\boldsymbol{\theta}}_r - K_r\int_{t-T_l(t)}^t \dot{\mathbf{q}}_l(\sigma)\, d\sigma.$$

Note that, since $\dot{\mathbf{q}}_l \in \mathcal{L}_2$,

$$\int_{t-T_l(t)}^t \dot{\mathbf{q}}_l(\sigma)\, d\sigma \leq {}^*T_r^{\frac{1}{2}}\|\dot{\mathbf{q}}_l\|_2 < \infty$$

(using Schwarz's inequality); hence, from (2b), it is proved that $\ddot{\boldsymbol{\theta}}_r \in \mathcal{L}_\infty$. This last, together with the fact that $\dot{\boldsymbol{\theta}}_r \in \mathcal{L}_2 \cap \mathcal{L}_\infty$ ensures that $\lim_{t\to\infty}|\dot{\boldsymbol{\theta}}_r(t)| = 0$. Moreover, since $\dot{\mathbf{q}}_i, \dot{\boldsymbol{\theta}}_r, \ddot{\boldsymbol{\theta}}_r \in \mathcal{L}_\infty$, it can be established that $\frac{d}{dt}\ddot{\boldsymbol{\theta}}_r \in \mathcal{L}_\infty$, which implies that $\ddot{\boldsymbol{\theta}}_r$ is uniformly continuous. This, along with the boundedness and existence of the following limit

$$\lim_{t\to\infty}\int_0^t \ddot{\boldsymbol{\theta}}_r(\sigma)\, d\sigma = -\dot{\boldsymbol{\theta}}_r(0) < \infty,$$

proves the claim that $|\ddot{\boldsymbol{\theta}}_r| \to 0$. This concludes the proof of Part I of Proposition 2.

In the rest of the proof, $\boldsymbol{\tau}_h$, $\boldsymbol{\tau}_e$ are both set to zero. In this case, the proof that $|\dot{\mathbf{q}}_l| \to 0$ is easily established noting that boundedness of $\dot{\mathbf{q}}_l$ and $|\mathbf{q}_l - \boldsymbol{\theta}_r|$ imply, from (1), that $\ddot{\mathbf{q}}_l \in \mathcal{L}_\infty$. Since $\dot{\mathbf{q}}_l \in \mathcal{L}_2 \cap \mathcal{L}_\infty$, $|\dot{\mathbf{q}}_l| \to 0$.

When $\boldsymbol{\tau}_h = \mathbf{0}$, (1) in closed-loop with (13a) can be written as

$$\ddot{\mathbf{q}}_l = -\mathbf{M}_l^{-1}\left([\mathbf{C}_l(\mathbf{q}_l, \dot{\mathbf{q}}_l) + B_l]\dot{\mathbf{q}}_l - K_l[\mathbf{q}_l - \boldsymbol{\theta}_r(t - T_r(t))]\right).$$

The fact that $\lim_{t\to\infty}|\dot{\mathbf{q}}_l(t)| = 0$ allows us to show that, if it is proved that $|\ddot{\mathbf{q}}_l| \to 0$, then the term $|\mathbf{q}_l - \boldsymbol{\theta}_r(t - T_r(t))| \to 0$. For, recall that with Properties P2, P3, P4 and boundedness of $\ddot{\mathbf{q}}_l$, $\dot{\mathbf{q}}_l$, $\dot{\boldsymbol{\theta}}_r$ and $|\mathbf{q}_l - \boldsymbol{\theta}_r|$ it can be shown that $\frac{d}{dt}\ddot{\mathbf{q}}_l \in \mathcal{L}_\infty$. On the other hand, $|\dot{\mathbf{q}}_l| \to 0$ implies that $\lim_{t\to\infty}\int_0^t \ddot{\mathbf{q}}_l(\sigma)\, d\sigma$ exists and it is finite. Hence, $|\ddot{\mathbf{q}}_l| \to 0$ as required.

[1] To avoid cluttering the notation, the argument of all time signals is omitted except for the case when it appears delayed.

[2] The assumption of scalar gains is made for simplicity, the case when these gains are positive definite diagonal matrices can be treated with slight modifications to the proof.

Now, using

$$\mathbf{q}_l - \boldsymbol{\theta}_r(t - T_r(t)) = \mathbf{q}_l - \boldsymbol{\theta}_r + \int_{t-T_r(t)}^{t} \dot{\boldsymbol{\theta}}_r(\sigma)d\sigma$$

together with convergence to zero of $\mathbf{q}_l - \boldsymbol{\theta}_r(t - T_r(t))$ and $\dot{\boldsymbol{\theta}}_r$, it is proved that $\lim_{t\to\infty} |\mathbf{q}_l - \boldsymbol{\theta}_r| = 0$. Rewriting (2b) in closed-loop with (13b) yields

$$\mathbf{J}_r\ddot{\boldsymbol{\theta}}_r = \mathbf{S}_r(\mathbf{q}_r - \boldsymbol{\theta}_r) + K_r(\mathbf{q}_l - \boldsymbol{\theta}_r) - K_r\int_{t-T_l(t)}^{t} \dot{\mathbf{q}}_l(\sigma)d\sigma - B_r\dot{\boldsymbol{\theta}}_r.$$

Note that convergence to zero of $\ddot{\boldsymbol{\theta}}_r$, $\dot{\boldsymbol{\theta}}_r$, $\dot{\mathbf{q}}_l$ and $|\mathbf{q}_l - \boldsymbol{\theta}_r|$ supports the claim that $\lim_{t\to\infty} |\mathbf{q}_r - \boldsymbol{\theta}_r| = 0$.

Finally, note that

$$\lim_{t\to\infty} |\mathbf{q}_l - \boldsymbol{\theta}_r| = \lim_{t\to\infty} |\mathbf{q}_l - \mathbf{q}_r + \mathbf{q}_r - \boldsymbol{\theta}_r| = 0$$

and $\lim_{t\to\infty} |\mathbf{q}_r - \boldsymbol{\theta}_r| = 0$; thus $\lim_{t\to\infty} |\mathbf{q}_l - \mathbf{q}_r| = 0$. This completes the proof. ◁

4.2. Dealing with local and remote flexibility

When the local manipulator exhibits joint flexibility, its dynamical behavior (1) transforms to

$$\mathbf{M}_l(\mathbf{q}_l)\ddot{\mathbf{q}}_l + \mathbf{C}_l(\mathbf{q}_l, \dot{\mathbf{q}}_l)\dot{\mathbf{q}}_l + \mathbf{S}_l[\mathbf{q}_l - \boldsymbol{\theta}_l] = \boldsymbol{\tau}_h \tag{16a}$$

$$\mathbf{J}_l\ddot{\boldsymbol{\theta}}_l + \mathbf{S}_l[\boldsymbol{\theta}_l - \mathbf{q}_l] = -\boldsymbol{\tau}_l \tag{16b}$$

where $\mathbf{J}_l \in \mathbb{R}^{n\times n}$ is a diagonal matrix corresponding to the local actuator inertia and $\mathbf{S}_l \in \mathbb{R}^{n\times n}$ is a diagonal and positive definite matrix that contains the local joint stiffness.

Proposition 3. *Consider the teleoperator (16) and (2), controlled by*

$$\boldsymbol{\tau}_l = K_l[\boldsymbol{\theta}_l - \boldsymbol{\theta}_r(t - T_r(t))] + B_l\dot{\boldsymbol{\theta}}_l \tag{17a}$$

$$\boldsymbol{\tau}_r = -K_r[\boldsymbol{\theta}_r - \boldsymbol{\theta}_l(t - T_l(t))] - B_r\dot{\boldsymbol{\theta}}_r \tag{17b}$$

with $\boldsymbol{\tau}_h$, $\boldsymbol{\tau}_e$ verifying (11). Set the control gains such that (14) holds. Then:

I. *All velocity signals and position errors are bounded, i.e., $\dot{\mathbf{q}}_i, \dot{\boldsymbol{\theta}}_i, \mathbf{q}_l - \mathbf{q}_r, \mathbf{q}_i - \boldsymbol{\theta}_i, \boldsymbol{\theta}_l - \boldsymbol{\theta}_r \in \mathcal{L}_\infty$. Moreover, $\dot{\boldsymbol{\theta}}_i \in \mathcal{L}_2$ and $|\ddot{\boldsymbol{\theta}}_i|, |\dot{\boldsymbol{\theta}}_i| \to 0$ as $t \to \infty$.*

II. *If additionally, the human operator and environment do not inject any forces on the local and remote manipulators, respectively, i.e. $\boldsymbol{\tau}_h = \boldsymbol{\tau}_e = \mathbf{0}$, the local and remote link position error and remote joint and actuator position error asymptotically converge to zero, i.e.,*

$$\lim_{t\to\infty} |\mathbf{q}_l(t) - \mathbf{q}_r(t)| = 0$$

and

$$\lim_{t\to\infty} |\mathbf{q}_i(t) - \boldsymbol{\theta}_i(t)| = 0.$$

Proof. The proof follows the same arguments as the proof of Proposition 2. Hence, only the main steps are presented here. Consider the function

$$W = W_l + \frac{K_l}{K_r}V_r + E_h + \frac{K_l}{K_r}E_e + \frac{K_l}{2}|\boldsymbol{\theta}_l - \boldsymbol{\theta}_r|^2$$

where W_l is similarly defined, for the local manipulator, as V_r in (3) by substituting the subscript r for l. E_h and E_e are defined in (11a) and (11b), respectively. Note that W is positive semi-definite and radially unbounded with regard to $\dot{\mathbf{q}}_i$, $\dot{\boldsymbol{\theta}}_i$, $|\mathbf{q}_i - \boldsymbol{\theta}_i|$ and $|\boldsymbol{\theta}_l - \boldsymbol{\theta}_r|$. Its time-derivative along (2), (16), (17), using Property P2 and (15), yields

$$\dot{W} = -B_l|\dot{\boldsymbol{\theta}}_l|^2 - K_l\dot{\boldsymbol{\theta}}_l^\top\int_{-T_r(t)}^{0} \dot{\boldsymbol{\theta}}_r(t+\sigma)d\sigma - \frac{K_lB_r}{K_r}|\dot{\boldsymbol{\theta}}_r|^2 - K_l\dot{\boldsymbol{\theta}}_r^\top\int_{-T_l(t)}^{0} \dot{\boldsymbol{\theta}}_l(t+\sigma)d\sigma.$$

Integrating from 0 to t, invoking Lemma 1 on the above integral terms, with α_l and α_r, respectively, yields $\lambda_l\|\dot{\boldsymbol{\theta}}_l\|_2^2 + \lambda_r\|\dot{\boldsymbol{\theta}}_r\|_2^2 \leq W(0)$, where λ_i are given, as in the previous proof, by $\lambda_l := B_l - \frac{K_l}{2}\left(\alpha_l + \frac{{}^*T_l^2}{\alpha_r}\right)$ and $\lambda_r := B_r - \frac{K_r}{2}\left(\alpha_r + \frac{{}^*T_r^2}{\alpha_l}\right)$. Hence, setting $4B_lB_r > ({}^*T_l + {}^*T_r)^2K_lK_r$ ensures that $\exists\alpha_i > 0$ such that $\lambda_i > 0$ and $\dot{\boldsymbol{\theta}}_i \in \mathcal{L}_2$, which in turn implies that $\dot{\mathbf{q}}_i$, $\dot{\boldsymbol{\theta}}_i$, $|\mathbf{q}_i - \boldsymbol{\theta}_i|$, $|\mathbf{q}_l - \boldsymbol{\theta}_r| \in \mathcal{L}_\infty$ and thus, $|\mathbf{q}_l - \mathbf{q}_r| \in \mathcal{L}_\infty$. Using these bounded signals, together with the expressions in (2), (16) and (17) it can be easily proved that $\lim_{t\to\infty} |\ddot{\boldsymbol{\theta}}_i(t)| = 0$ and $\lim_{t\to\infty} |\dot{\boldsymbol{\theta}}_i(t)| = 0$. This completes Part I of the proof.

For the proof of Part II, we set $\boldsymbol{\tau}_h = \boldsymbol{\tau}_e = \mathbf{0}$ and, hence, dynamics (16a) and (2a) can be both written as

$$\ddot{\mathbf{q}}_i = -\mathbf{M}_i^{-1}\left(\mathbf{C}_i(\mathbf{q}_i, \dot{\mathbf{q}}_i)\dot{\mathbf{q}}_i - \mathbf{S}_i[\mathbf{q}_i - \boldsymbol{\theta}_i]\right).$$

Now, the fact that $\dot{\mathbf{q}}_i$, $|\mathbf{q}_i - \boldsymbol{\theta}_i| \in \mathcal{L}_\infty$ ensure that $\ddot{\mathbf{q}}_i \in \mathcal{L}_\infty$ and Barbălat's Lemma supports that $\lim_{t\to\infty} |\dot{\mathbf{q}}_i(t)| = 0$. This last, together with convergence to zero of $\ddot{\mathbf{q}}_i$ ensure that $|\mathbf{q}_i - \boldsymbol{\theta}_i| \to 0$ which in turn implies, from (16b), that $|\boldsymbol{\theta}_l(t) - \boldsymbol{\theta}_r(t - T_r(t))| \to 0$. Now, $|\dot{\mathbf{q}}_i| \to 0$ implies that $\lim_{t\to\infty}\int_0^t \ddot{\mathbf{q}}_i(\sigma)d\sigma$ exists and it is finite. Moreover, the boundedness of $\ddot{\mathbf{q}}_i$, $\dot{\mathbf{q}}_i$, $\dot{\boldsymbol{\theta}}_i$, together with P4, ensures that $\ddot{\mathbf{q}}_i$ is uniformly continuous. Hence $|\ddot{\mathbf{q}}_i| \to 0$. Finally,

$$\mathbf{q}_l - \mathbf{q}_r = \mathbf{q}_l - \boldsymbol{\theta}_l + \boldsymbol{\theta}_l - \boldsymbol{\theta}_r(t - T_r(t)) - \mathbf{q}_r + \boldsymbol{\theta}_r - \int_{t-T_r(t)}^{t} \dot{\boldsymbol{\theta}}_r(\sigma)d\sigma,$$

and convergence to zero of $|\mathbf{q}_i - \boldsymbol{\theta}_i|$, $|\boldsymbol{\theta}_l - \boldsymbol{\theta}_r(t - T_r(t))|$ and $|\dot{\boldsymbol{\theta}}_r|$ supports the claim that $\lim_{t\to\infty} |\mathbf{q}_l - \mathbf{q}_r| = 0$. This completes the proof. ◁

Remark 4. Recently, the authors of this paper have proposed a solution to the position tracking problem for rigid bilateral teleoperators with variable time-delays and with unmeasured velocities [31]. An immersion and invariance (I&I) observer from [32] is proposed in order to obtain a globally exponentially convergent estimate of the unmeasured velocities. Through a Lyapunov-like analysis, it has been shown that this observer, in conjunction with a simple $P + d$ controller, ensures the global boundedness of the closed-loop trajectories while, in the absence of external forces acting on the system, position coordination with zero velocities has been established. This result can be straightforwardly extended to the case of bilateral teleoperators with time-delays and flexibility (either for one or both manipulators) in closed-loop with the $P + d$ controllers of Section 4. This is due to the fact that the analysis presented in [31] does not need any modification in order to treat the flexibility effects, since the design framework naturally includes this case.

5. Simulations

To show the effectiveness of the proposed control schemes, some simulations, in which the local and remote manipulators are modeled as a pair of 2 DOF serial links with revolute joints (see Fig. 2), have been performed. The teleoperator is composed of a rigid local manipulator and a remote manipulator with flexible joints. The corresponding nonlinear dynamics is modeled by (1) and (2). In what follows, $\alpha_i := l_{2_i}^2 m_{2_i} + l_{1_i}^2(m_{1_i} + m_{2_i})$, $\beta_i := l_{1_i}l_{2_i}m_{2_i}$

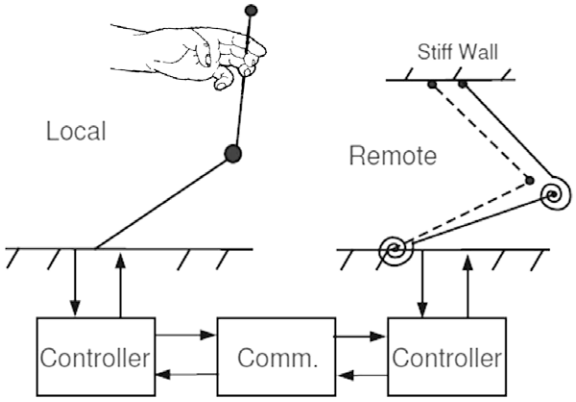

Fig. 2. Simulations test-bed.

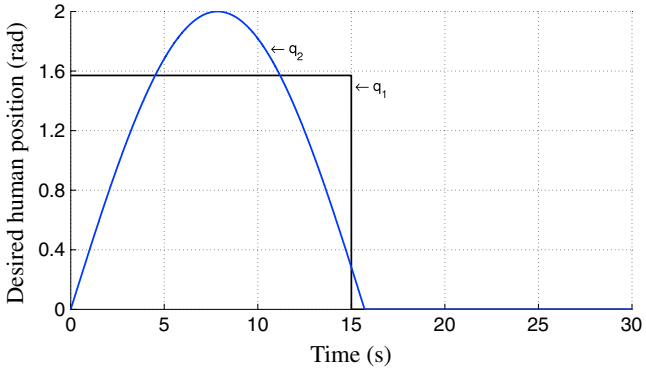

Fig. 3. Desired human position for the spring-damper model.

and $\delta_i := l_{2_i}^2 m_{2_i}$, with l_{k_i} and m_{k_i} being, respectively, the length and mass of link k of manipulator i, with $k \in \{1, 2\}$. The inertia matrices $\mathbf{M}_i(\mathbf{q}_i)$ are given by

$$\mathbf{M}_i(\mathbf{q}_i) = \begin{bmatrix} \alpha_i + 2\beta_i c_{2_i} & \delta_i + \beta_i c_{2_i} \\ \delta_i + \beta_i c_{2_i} & \delta_i \end{bmatrix},$$

where c_{2_i} is the short notation for $\cos(q_{2_i})$ being q_{2_i} the position of link 2 of manipulator i. The Coriolis and centrifugal effects are modeled by

$$\mathbf{C}_i(\mathbf{q}_i, \dot{\mathbf{q}}_i) = \begin{bmatrix} -\beta_i s_{2_i} \dot{q}_{2_i} & -\beta_i s_{2_i} (\dot{q}_{1_i} + \dot{q}_{2_i}) \\ \beta_i s_{2_i} \dot{q}_{1_i} & 0 \end{bmatrix},$$

where s_{2_i} is the short notation for $\sin(q_{2_i})$ while $\dot{q}_{1_i}$, $\dot{q}_{2_i}$ are the respective revolute velocities of the two links. The remote actuator inertia is given by $\mathbf{J}_r = 0.3\mathbf{I}$ kg m$^2 \in \mathbb{R}^{2\times 2}$ and the stiffness of the remote flexible joints is $\mathbf{S}_r = 100\mathbf{I}$ N m $\in \mathbb{R}^{2\times 2}$.

The physical parameters for the manipulators are: links length $l_{1_i} = l_{2_i} = 0.38$ m; masses of the links $m_{1_l} = 3.947368$ kg, $m_{2_l} = 0.62326$ kg, $m_{1_r} = 0.5$ kg and $m_{2_r} = 0.35$ kg. The initial conditions are $\hat{\boldsymbol{\phi}}_l(0) = \dot{\mathbf{q}}_l(0) = \dot{\boldsymbol{\theta}}_r(0) = \boldsymbol{\theta}_r(0) = \mathbf{0}$, $\mathbf{q}_l^\top(0) = [-1, 1]^\top$ rad and $\mathbf{q}_r^\top(0) = [-0.1, 0.1]^\top$ rad. The human operator is modeled as a spring-damper system, i.e., $\boldsymbol{\tau}_h = K_s[\mathbf{q}_h - \mathbf{q}_l] - K_d\dot{\mathbf{q}}_l$ (where $\mathbf{q}_h$ is the desired trajectory for the human operator and it is shown in Fig. 3), with gains $K_s = 10$ N m and $K_d = 2$ N m s.

Two sets of simulations are presented, one using the asymmetric controller in Section 3 and another using the symmetric controller of Section 4.1.

For the adaptive controller of Section 3, the matrix $\mathbf{Y}_l$ is given by

$$\mathbf{Y}_l = \begin{bmatrix} \dot{e}_{1_l} & Y_{12} & \dot{e}_{2_l} \\ 0 & c_{2_l}\dot{e}_{1_l} + s_{2_l}\dot{q}_{1_l}e_{1_l} & \dot{e}_{1_l} + \dot{e}_{2_l} \end{bmatrix}$$

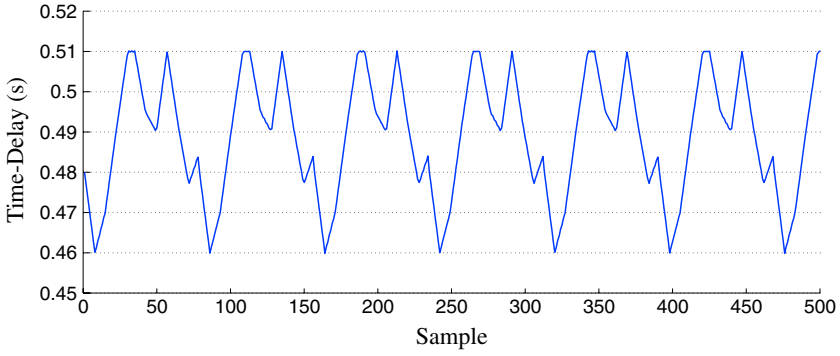

Fig. 4. Variable time-delay used in the simulations of the $P + d$ controller.

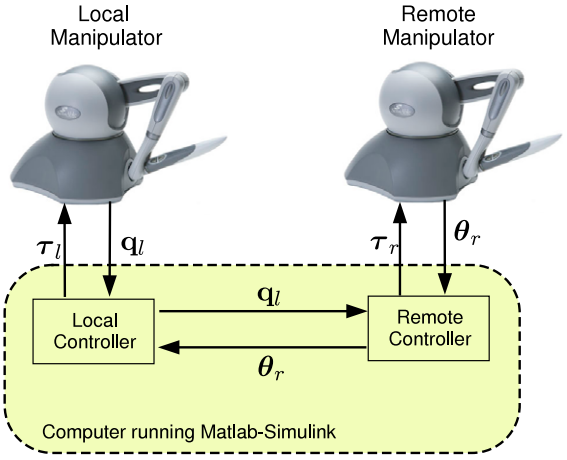

Fig. 5. Experimental setup, composed of two PHANToM Omni® devices.

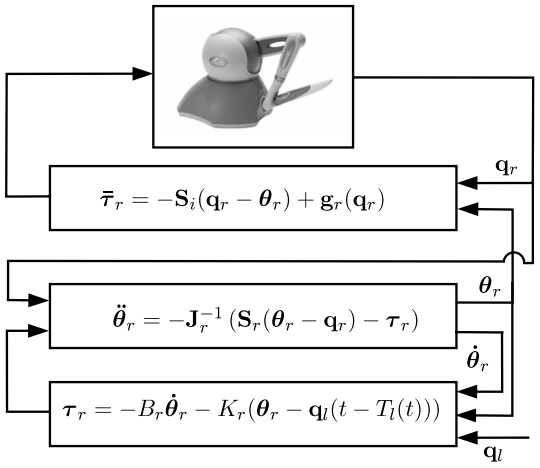

Fig. 6. Emulated remote flexible-joint manipulator.

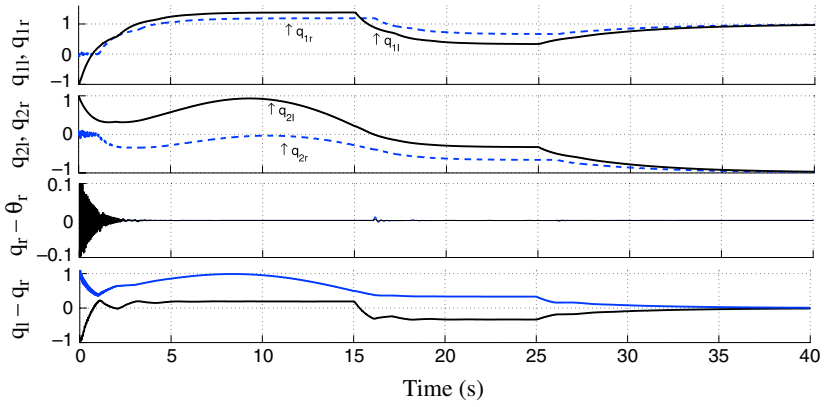

Fig. 7. Local and remote link positions, remote link-joint error and local and remote link position errors in the free space using the adaptive controller.

where $Y_{12} = 2c_{2_l}\dot{e}_{1_l} + c_{2_l} + \dot{e}_{2_l} - s_{2_l}(\dot{q}_{1_l} + \dot{q}_{2_l})e_{2_l} - s_{2_l}\dot{q}_{2_l}e_{1_l}$. The estimated physical parameters are $\hat{\boldsymbol{\phi}}_l = \begin{bmatrix}\hat{\alpha}_l & \hat{\beta}_l & \hat{\delta}_l\end{bmatrix}^\top$.

The control gains, for the asymmetric scheme, are: $\lambda = 1$, $\boldsymbol{\Gamma}_l = \mathbf{I}$, $\mathbf{K}_l = 10\mathbf{I}$, $\mathbf{K}_r = 5\mathbf{I}$ N m s and $\mathbf{B} = 5\mathbf{I}$ N m s. These values satisfy that the gains have to be positive definite, and symmetric. For simplicity, in these simulations, the time-delay in both directions has been set to 1 s, i.e., $T_l = T_r = 1$ s.

The first set of simulations presents the results using the asymmetric controller of Section 3, when both local and remote manipulators move freely in space. Fig. 7 shows the local and the remote joint positions, and remote joint-actuator position error together with the local and remote position errors. The asymptotic behavior of both local and remote position errors, and remote joint-actuator position error can be clearly observed, i.e., convergence to zero of $|\mathbf{q}_l - \mathbf{q}_r|$ and $|\boldsymbol{\theta}_r - \mathbf{q}_r|$. Fig. 8 depicts the time evolution of the estimated parameters $\hat{\boldsymbol{\phi}}_l$, and it is observed that these values remain bounded, as stated in Proposition 1. Note that joint position error asymptotically converges to zero despite the constant time-delays.

The second set of simulations has been performed using the symmetric $P + d$ controller of Section 4.1, in (13). The gains are: $K_l = 5$ N m, $B_l = 5$ N m s, $K_r = 10$ N m and $B_r = 7$ N m s. These gains have been set according to (14). The simulations of this scheme are in free space and interacting with a stiff virtual wall. This wall is modeled as a spring-damper system with stiffness equal to 20,000 Nm and damping equal to 200 N m s, located at 0.5 m in the y-coordinate. The upper bound, for the variable time-delays used in this set of simulations, is ${}^*T_i = 0.55$ s (Fig. 4).

The free space simulations are shown in Fig. 9. Note that the position error asymptotically converges to zero despite the variable time-delays. Fig. 10, on the other hand, depicts the joint position time evolution when interacting with the stiff wall while Fig. 11 shows the same results in Cartesian space. In this last figure, it can be clearly seen that, around 2.5 s, the remote manipulator comes in contact with the wall and, around 17.5 s, it retracts from the wall. Despite the stiff interaction, both, local and remote link position errors and remote actuator and link position error converge to zero.

6. Experiments

This section presents, in the same spirit as the previous section, some experimental results that show the effectiveness of the proposed controllers. The experiments have been performed using the symmetric $P+d$ controller of Section 4.1. The local and remote manipulators are two 3-DOF mechanical systems. These devices are the PHANToM Omni trademark of Sensable Technologies (http://sensable.com/). The software runs in the same computer and the devices are cascade connected through a Firewire 1934 port. Fig. 5

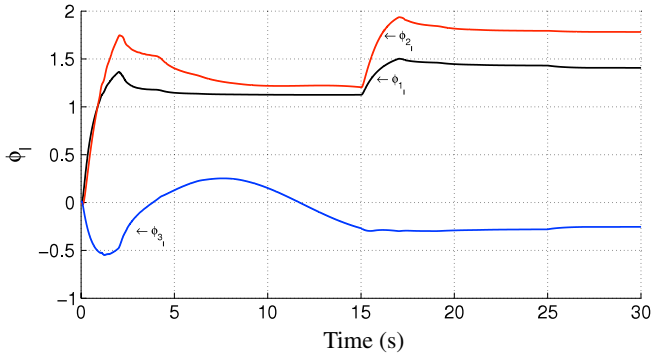

Fig. 8. Time evolution of the estimated parameters for the asymmetric adaptive controller.

shows the experimental setup. The controllers and all software are implemented in Matlab Simulink® The communication between Simulink and the Omni devices is done using the *PhanTorque* and the *OmniTorque* libraries, which have been developed by the authors.[3] An induced time-delay has been implemented similar to that in Fig. 4 and ${}^*T_i = 0.55$ s.

The compensated gravity vector is given by

$$\mathbf{g}_i(\mathbf{q}_i) = \begin{bmatrix} 0 \\ \phi_1 \sin(q_2 + q_3) + \phi_2 \cos(q_2) \\ \phi_1 \sin(q_2 + q_3) \end{bmatrix},$$

where $\phi_1 = gm_3l_2$, $\phi_2 = gm_3l_2 + gm_2l_1$ and g is the acceleration of gravity constant. These physical values have been experimentally estimated yielding $\phi_1 = 0.0095$ kg m and $\phi_2 = 0.0127$ kg m.

Since the 3-DOFs of the PHANToM Omni® devices are fully-actuated, this paper emulates a remote flexible-joint (under-actuated) behavior by using the control scheme in Fig. 6. The closed-loop behavior of such a system corresponds to that of (2) in closed-loop with (13). In this case, the motor inertia matrix has been set to $\mathbf{J}_r = \text{diag}(0.25, 0.15, 0.1)$ and the joint stiffness matrix is set to $\mathbf{S}_r = 0.9\mathbf{I}_3$. It should be noted that the initial conditions of the actuated and the non-actuated positions differ one from another, that is, $\mathbf{q}_r(0) \neq \boldsymbol{\theta}_r(0)$.

Both, local and remote, proportional gains have been set as $K_i = 0.4$ and, in order to fulfill (14), the damping gains have been set to $B_i = 0.5$.

Two different experiments have been carried out. The first corresponds to the case when only the remote manipulator exhibits joint-flexibilities and the second deals with local and remote

[3] The *PhanTorque* and the *OmniTorque* libraries are publicly available at https://sir.upc.edu/wikis/roblab/index.php/Projects/PhanTorqueLibraries.

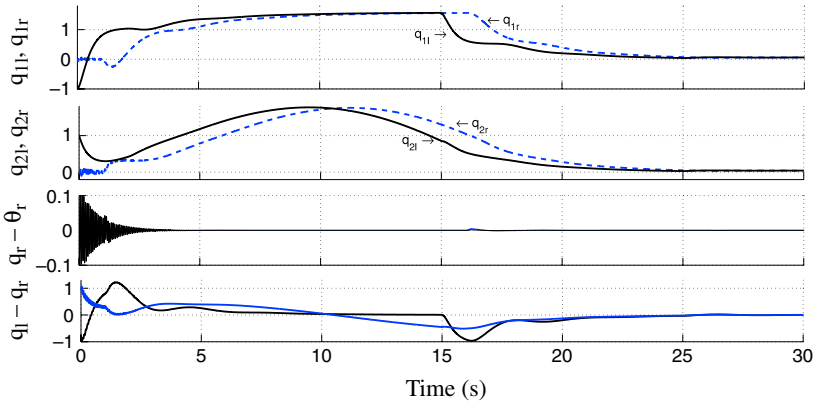

Fig. 9. Link position results using the $P + d$ controller in the free space.

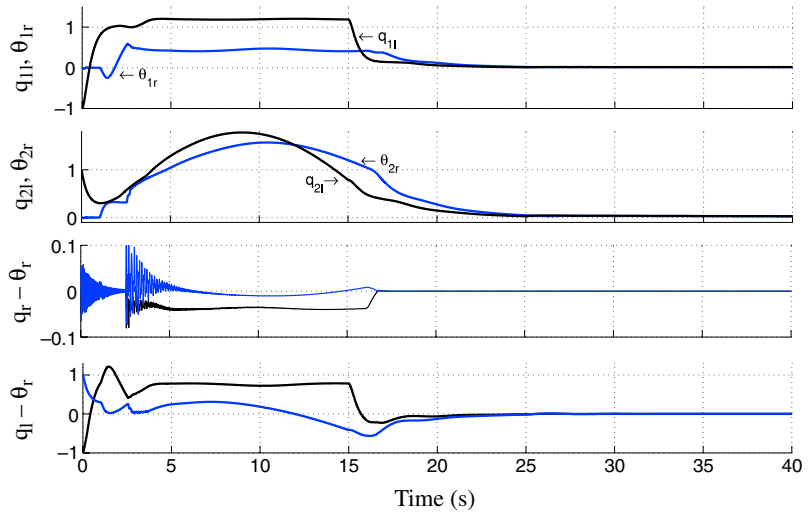

Fig. 10. Joint position tracking using the $P + d$ scheme while interacting with a stiff wall.

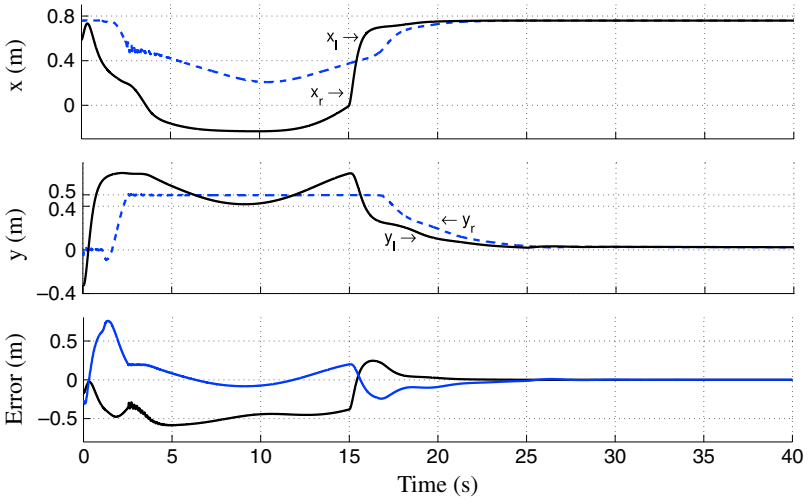

Fig. 11. Cartesian space results using the $P + d$ controller while interacting with a stiff wall, located at the coordinate $y = 0.5$ m.

flexibility. Fig. 12 shows the tracking performance of the $P+d$ controller and Fig. 13 depicts the error of the remote joint and link angular positions. Note that when the human operator interacts with the local manipulator, from 4 to 23 s, the position error is bounded and when the human releases the local manipulator, from 23 s, the position error asymptotically converges to zero. Figs. 14 and 15 present the experimental results for the second case. For simplicity, the local motor inertia and joint stiffness have been set equal to those of the remote manipulator. Even with local and remote joint-flexibility, the link position error remains bounded when the human interacts with the local manipulator, from 5 to 23 s, and the error asymptotically converges to zero otherwise.

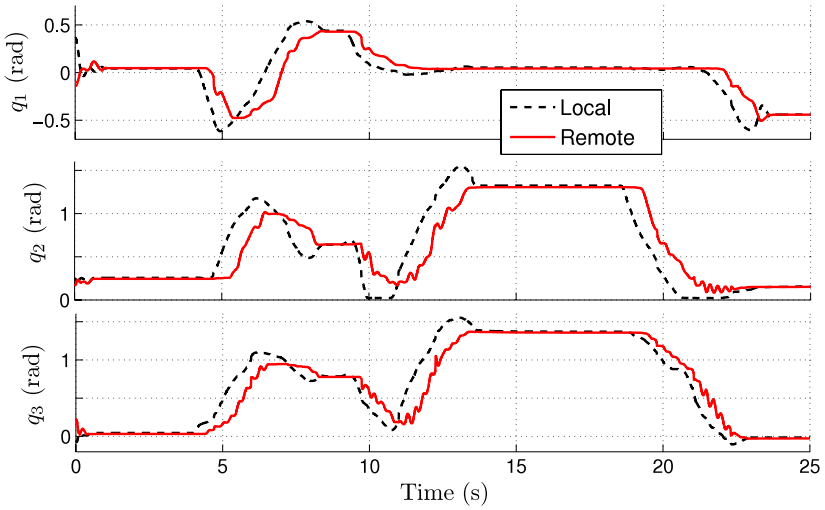

Fig. 12. Experimental behavior of the, local and remote, link positions when only the remote manipulator exhibits joint-flexibility.

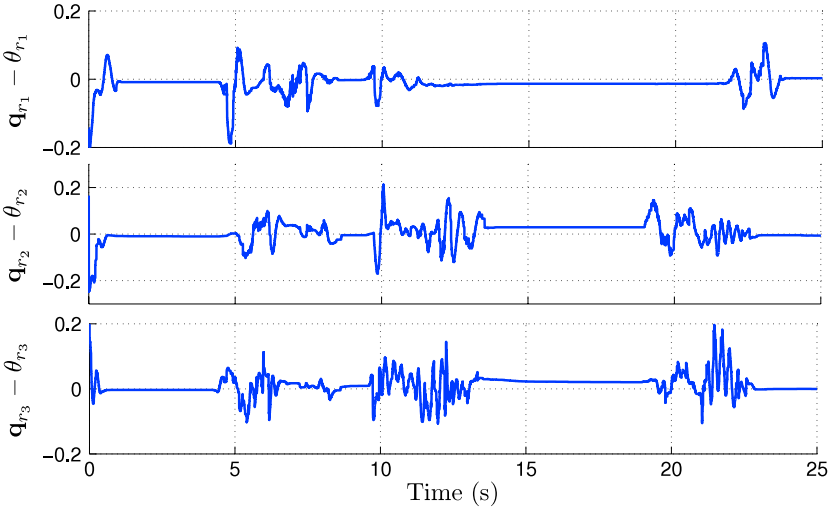

Fig. 13. Position error between the actuated and the non-actuated positions of the remote manipulator, i.e., $\mathbf{q}_r - \boldsymbol{\theta}_r$.

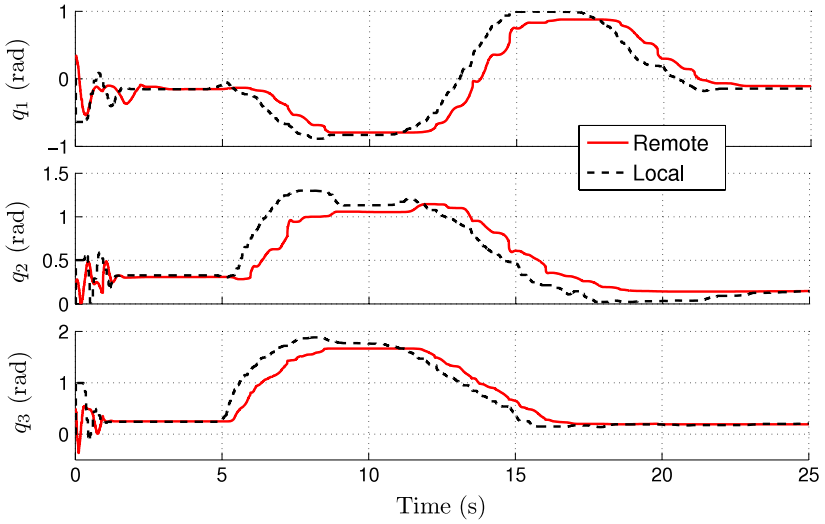

Fig. 14. Experimental behavior of the, local and remote, link positions when both manipulators exhibit joint-flexibility.

7. Conclusions

This paper proposes two control schemes, asymmetric and symmetric, that can achieve asymptotic convergence to zero of the local and remote position errors for nonlinear teleoperators with flexible joint manipulators. Without using strict Lyapunov functions but with the application of the Barbalăt's Lemma and some signal bounding, convergence of position error and velocities to

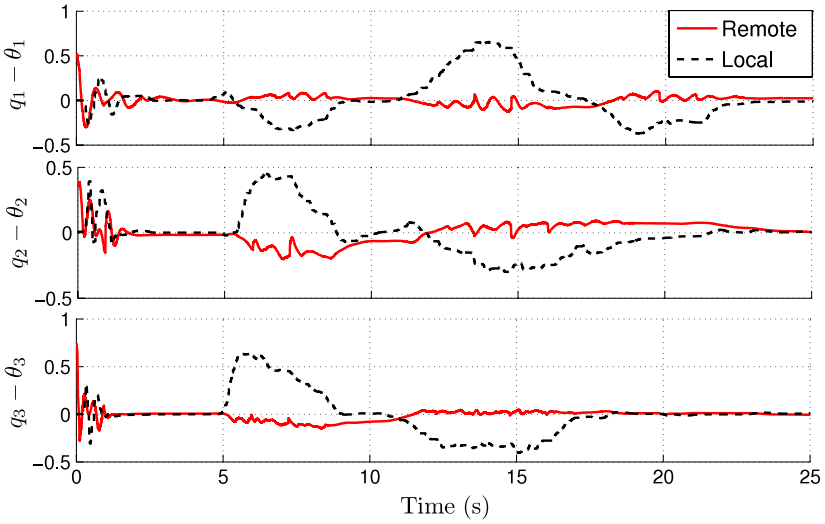

Fig. 15. Position error between the actuated and the non-actuated positions of the local and the remote manipulators.

zero is established even in the presence of joint flexibility and variable time-delays. The theoretical results are supported by simulations with a rigid local manipulator and a flexible joint remote manipulator, some of them accounting for an interaction with a stiff virtual wall. Experimental results, using a couple of 3-DOF devices, show the performance of the $P+d$ controllers in two different cases, with only remote joint-flexibility and with local and remote flexibility.

Moreover, the recent results on the output–feedback tracking for nonlinear bilateral teleoperators, obtained by the same authors, can be directly extended to the case with flexibility effects. In this way, an explicit solution is provided to the problem of finding a (dynamic) stabilizing controller for a general nonlinear teleoperator that uses only (local) position measurements, while taking into account the practical limitations due to communication delays and joint flexibility.

Current work is under way to propose a more general framework by proving position tracking in the case where gravity and quantization effects are also included in the control design. The gravity cancelation term is designed using a similar scheme as that in [33], which studies the consensus problem in networks of multiple flexible-joint manipulators, and originally proposed in [34].

References

[1] P. Hokayem, M. Spong, Bilateral teleoperation: an historical survey, Automatica 42 (12) (2006) 2035–2057.
[2] E. Nuño, L. Basañez, R. Ortega, Passivity-based control for bilateral teleoperation: a tutorial, Automatica 47 (3) (2011) 485–495.
[3] R. Anderson, M. Spong, Bilateral control of teleoperators with time delay, IEEE Trans. Automat. Control 34 (5) (1989) 494–501.
[4] N. Chopra, M. Spong, R. Ortega, N. Barabanov, On tracking preformance in bilateral teleoperation, IEEE Trans. Robot. 22 (4) (2006) 844–847.
[5] N. Chopra, M. Spong, R. Lozano, Synchronization of bilateral teleoperators with time delay, Automatica 44 (8) (2008) 2142–2148.
[6] E. Nuño, R. Ortega, L. Basañez, An adaptive controller for nonlinear teleoperators, Automatica 46 (1) (2010) 155–159.
[7] E. Nuño, R. Ortega, L. Basañez, Erratum to: an adaptive controller for nonlinear teleoperators [Automatica 46 (2010) 155-159], Automatica 47 (5) (2011) 1093–1094.
[8] E. Nuño, R. Ortega, L. Basañez, D. Hill, Synchronization of networks of nonidentical Euler–Lagrange systems with uncertain parameters and communication delays, IEEE Trans. Automat. Control 56 (4) (2011) 935–941.
[9] S. Salcudean, M. Zhu, W. Zhu, K. Hashtrudi-Zaad, Transparent bilateral teleoperation under position and rate control, Int. J. Robot. Res. 19 (12) (2000) 1185–1202.
[10] W. Zhu, S. Salcudean, Stability guaranteed teleoperation: an adaptive motion/force control approach, IEEE Trans. Automat. Control 45 (11) (2000) 1951–1969.
[11] S. Sirouspour, Modeling and control of cooperative teleoperation systems, IEEE Trans on Robotics 21 (6) (2005) 1220–1225.
[12] D. Lee, M. Spong, Passive bilateral teleoperation with constant time delay, IEEE Trans. Robot. 22 (2) (2006) 269–281.
[13] E. Nuño, R. Ortega, N. Barabanov, L. Basañez, A globally stable PD controller for bilateral teleoperators, IEEE Trans. Robot. 24 (3) (2008) 753–758.
[14] E. Nuño, L. Basañez, R. Ortega, M. Spong, Position tracking for nonlinear teleoperators with variable time-delay, Int. J. Robot. Res. 28 (7) (2009) 895–910.
[15] M. Mahvash, P. Dupont, Stiffness control of surgical continuum manipulators, IEEE Trans. Robot. 27 (2) (2011) 334–345.
[16] M. Tavakoli, R.D. Howe, Haptic effects of surgical teleoperator flexibility, Int. J. Robot. Res. 28 (10) (2009) 1289–1302.
[17] M. Tavakoli, R. Howe, The effect of joint elasticity on bilateral teleoperation, in: 2007 IEEE/RSJ Int. Conf. Intelligent Robots and Systems, 2007, pp. 1618–1623.
[18] D. Moschini, P. Fiorini, Performance of robotic teleoperation system with flexible slave device, in: 2004 IEEE Int. Conf. Robotics and Automation, 2004, pp. 3696–3701.
[19] Y. Morita, H. Marumo, M. Uchida, T. Mori, H. Ukai, H. Kando, Assist control method for positioning task using master–slave manipulators with flexibility on slave arm, in: 2007 IEEE International Conference on Control Applications. 2007, pp. 232–237.
[20] M. Mahvash, P. Dupont, Bilateral teleoperation of flexible surgical robots, in: Chopra N., Peer A., Secchi C., Ferre M., editors. IEEE ICRA 2008 Workshop: New Vistas and Challenges in Telerobotics. Pasadena, CA, USA; 2008, pp. 58–64.
[21] A. Tobergte, A. Albu-Schäffer, Direct force reflecting teleoperation with a flexible joint robot, in: IEEE Int. Conf. on Robotics and Automation. St. Paul, Minnesota; 2012, pp. 4280–4287.
[22] E. Nuño, I. Sarras, L. Basañez, M. Kinnaert, A proportional plus damping injection controller for teleoperators with joint flexibility and time-delays, in: IEEE Int. Conf. on Robotics and Automation. St. Paul, Minnesota; 2012, pp. 4294–4299.
[23] P. Tomei, A simple PD controller for robots with elastic joints, IEEE Trans. Automat. Control 36 (10) (1991) 1208–1213.
[24] R. Kelly, V. Santibanez, Global regulation of elastic joint robots based on energy shaping, IEEE Trans. Automat. Control 43 (10) (1998) 1451–1456.
[25] F. Ghorbel, B. Srinivasan, M. Spong, On the uniform boundedness of the inertia matrix of serial robot manipulators, J. Robot. Syst. 15 (1) (1998) 17–28.
[26] I. Duleba, Structural properties of inertia matrix and gravity vector of dynamics of rigid manipulators, J. Robot. Syst. 19 (11) (2002) 555–567.
[27] R. Gunawardana, F. Ghorbel, On the uniform boundedness of the coriolis/centrifugal terms in the robot equations of motion, Int. J. Robot. Autom. 14 (2) (1999) 45–53.
[28] R. Kelly, V. Santibáñez, A. Loria, Control of robot manipulators in joint space, in: Advanced Textbooks in Control and Signal Processing, Springer-Verlag, ISBN: 1-85233-994-2, 2005.
[29] M. Spong, S. Hutchinson, M. Vidyasagar, Robot Modeling and Control, Wiley, ISBN: 978-0-471-64990-8, 2005.
[30] P. Ioannou, B. Fidan, Adaptive Control Tutorial, in: SIAM Advances in Design and Control, 2006.
[31] I. Sarras, E. Nuño, M. Kinnaert, L. Basañez, Output-feedback control of nonlinear bilateral teleoperators, in: IEEE American Control Conference, Montreal, Canada; 2012, pp. 3490–3495.
[32] A. Astolfi, R. Ortega, A. Venkatraman, A globally exponentially convergent immersion and invariance speed observer for mechanical systems with nonholonomic constraints, Automatica 46 (1) (2010) 182–189.
[33] E. Nuño, D. Valle, I. Sarras, L. Basañez, Leader–follower and leaderless consensus in networks of flexible–joint manipulators with delays, Eur. J. Control 20 (5) (2014) 249–258.

[34] A. De Luca, B. Siciliano, L. Zollo, PD control with on-line gravity compensation for robots with elastic joints: theory and experiments, Automatica 41 (10) (2005) 1809–1819.

Emmanuel Nuño was born in Guadalajara, México, in 1980. He obtained his B.Sc. in Communications and Electronics Engineering from the University of Guadalajara in 2002. He received the Ph.D. degree in Electrical Engineering from the Technical University of Catalonia (UPC), Spain, in July 2008.

In 2007 he held two research internships, at the Laboratoire des Signaux et Systemes at SUPELEC and at the Coordinated Science Laboratory at University of Illinois, Urbana-Champaign. From Nov. 2009 through Oct. 2010 he was a posdoctoral researcher at the Institute of Industrial and Control Engineering (IOC) at the Technical University of Catalonia. In 2008 he joined the Department of Computer Science of the University of Guadalajara.

His research interests include nonlinear control of robot manipulators, control of teleoperators with time-delays and synchronization of multiple Euler–Lagrange systems.

Ioannis Sarras was born in Athens, Greece, in 1982. He graduated from the Automation Engineering Department of the Technological Education Institute (T.E.I.) of Piraeus in 2004 and received the Master of Research (M2R) in Control Theory from the University of Paul Sabatier (Toulouse III) in 2006, with scholarship from the General Michael Arnaoutis Foundation. He obtained the Ph.D. degree with distinction in Control Theory with applications on mechanical systems from the university of Paris-Sud XI, France, in 2010 with a scholarship from the Greek Scholarships Foundation. From June 2010 till September 2011, he was a researcher at the Université Libre de Bruxelles and actually, he is working at the Laboratory of Signals and Systems (LSS) of the National Center for Scientific Research (CNRS). He has been a visiting researcher for short and long term periods at the university of Groningen (the Netherlands), the Technical University of Catalunia (Spain), the university of Seville (Spain) and the Indian Institutes of Technology in Bombay and in Madras (India). His research interests are in the fields of nonlinear control and Lyapunov analysis with emphasis on telerobotics and (networks of) mechanical systems.

Luis Basañez received the Ph.D. degree in Electrical Engineering from the Technical University of Catalonia (UPC), Barcelona, Spain, in 1975. From 1976 to 1987, he was the Vice Director of the Institute of Cybernetics (UPC), where he was the Director from 1987 to 1990. Since 1986, he has been a Full Professor of System Engineering and Automatic Control at the UPC, where since 1990 he is the Head of the Robotics Division, Institute of Industrial and Control Engineering. His current research interests include task planning, multirobot systems coordination, teleoperation, sensor integration, and active perception.

Dr. Basañez was an Executive Committee Member of the International Federation of Robotics (IFR) from 1987 to 1992, and he is currently the Spanish delegate at the IFR. In 2005, he was an elected Fellow of the International Federation of Automatic Control (IFAC), and since this year, he is a Member of the IFAC Council.

Michel Kinnaert graduated in 1983 from «Université libre de Bruxelles» (ULB), Brussels, Belgium, in Mechanical and Electrical Engineering. He received the M.S. degree in Electrical Engineering from Stanford University in 1984, and the Ph.D. degree from ULB in 1987. After being employed for 6 years by the Belgian National Fund for Scientific Research, he was appointed by ULB where he is now Professor in the Department of Control Engineering and System Analysis. He held visiting professor positions in "Université Claude Bernard Lyon I", Lyon, France. He has been chairman of the IFAC Technical Committee SAFEPROCESS from 2002 to 2008 and he is an associate editor of the IFAC Journal Control Engineering Practice since 2005. He co-authored, with M. Blanke, J. Lunze and M. Staroswiecki, the book Diagnosis and Fault Tolerant Control—Second Edition, Springer, 2006.

His research interests include fault detection and isolation and fault tolerant control, with applications in the process industry, power systems and mechatronics.